Building and Environment 261 (2024) 111757

Contents lists available at ScienceDirect

Building and Environment

journal homepage: www.elsevier.com/locate/buildenv

Novel MOF-based autonomous humidity control materials for energy-efficient indoor moisture regulation

Menghao Qin [a,*], Oliver S. Rasmussen [a], Jun Chen [b], Lars Wadsö [c]

[a] Department of Environmental and Recourse Technology, Technical University of Denmark, 2800, Lyngby, Denmark
[b] Department of Chemistry, Technical University of Denmark, 2800, Lyngby, Denmark
[c] Division of Building Materials, LTH, Lund University, 22100, Lund, Sweden

ARTICLE INFO

Keywords:
Autonomous humidity control material
Metal-organic framework
Moisture control
Building energy saving

ABSTRACT

The concept of autonomous humidity control material (AHCM) is inspired by phase change material. AHCM is a new type of functional sorbent material. It can adsorb/release sufficient water vapor at the target relative humidity level and autonomously maintain the indoor relative humidity at a set value/range without external intervention, which cannot be achieved by conventional sorbents (e.g., zeolite, silica gel, etc.). In this study, a novel metal-organic framework (MOF) based AHCM is prepared, and its application for energy-efficient indoor moisture control has been investigated. The new MOF-AHCM has an S-shaped water vapor isotherm, large porosity, and high moisture adsorption capacity. The trigger points for adsorption and desorption occur at 60 % and 40 % RH, respectively. It means MOF-AHCM can autonomously regulate the indoor relative humidity to fall within 40%–60 % RH, which fits the thermal comfort range recommended by ASHRAE well. The physicochemical and hygrothermal characteristics of the synthesized MOF-ACHM have been assessed. Full-scale chamber tests were carried out to verify the humidity control ability of the new material. The experimental results show that MOF-AHCM can significantly mitigate indoor humidity fluctuation and regulate the humidity level within the target range autonomously. Furthermore, numerical simulation has been performed to investigate the impact of MOF-AHCM on building energy consumption in different moisture regions globally, namely, arid, semiarid, dry, moist, and wet areas. The results reveal that MOF-AHCM has an excellent humidity control capacity and can reduce the latent cooling demand of HVAC systems in most climates, especially in arid, semiarid, dry, and moist areas.

1. Introduction

The growing demand for moisture control in buildings is one of the most critical blind spots in today's energy analysis for carbon neutrality in building operations. Global warming not only raises temperatures but also intensifies the water cycle, leading to heightened evaporation and altered precipitation patterns [1]. These combined factors accelerate the rise of humidity in the air. The latent cooling (dehumidification) load currently makes up around one-third of the total energy demand of an HVAC system, and it will quickly increase in the coming decades [2]. Relative humidity also affects the health of occupants and may increase the occurrence of respiratory diseases and allergies [3]. There are three common methods for moisture control: refrigeration dehumidification, solid desiccant dehumidification, and liquid sorbent dehumidification. Conventional air conditioners use refrigeration dehumidification to remove the latent cooling load. However, this process is energy inefficient as the air is first cooled to the dew point and then re-heated to the desired indoor temperature [4]. Solid desiccant systems provide independent control over temperature and humidity, helping to reduce energy consumption [5,6]. Zeolites and silica gels are the commonly used desiccants. However, they are inefficient for indoor humidity control due to the high energy demand for regeneration, low water vapor uptake, and long cycle time. More importantly, owning to the inherent characteristics of their isotherms, most of their moisture adsorption occurs outside the desired RH range, and neither silica gel nor zeolite can precisely control indoor humidity within the required range (for example, 40 %–60 % RH for indoor thermal comfort) [7]. Conventional hygroscopic building materials (e.g., wood, gypsum, etc.) also have a certain ability of moisture buffering [8–10]. However, their adsorption capacity is very limited compared to solid desiccants. In order to

* Corresponding author.
E-mail address: menqin@dtu.dk (M. Qin).

https://doi.org/10.1016/j.buildenv.2024.111757
Received 29 February 2024; Received in revised form 24 May 2024; Accepted 17 June 2024
Available online 18 June 2024
0360-1323/© 2024 The Authors. Published by Elsevier Ltd. This is an open access article under the CC BY license (http://creativecommons.org/licenses/by/4.0/).

moderate the indoor RH variations, a large number of materials are needed to cover most internal surfaces, which is not practical in many cases. Like conventional solid desiccants, these hygroscopic building materials are unable to precisely control indoor humidity. Liquid sorbent dehumidification consumes less electricity compared to refrigeration. However, the technology has notable drawbacks that hinder its commercialization in building applications. These include complex and large systems, as well as issues with corrosion [11].

Developing novel functional sorbent materials, such as autonomous humidity control material (AHCM) for energy-efficient indoor moisture control, has gradually attracted the attention of many researchers from both building science and chemistry [12,13]. The basic concept of AHCM is derived from the principle of phase change materials (PCM). PCMs can absorb/release significant amounts of thermal energy at a constant temperature (i.e., melting point or solidification point) during their phase change process and can be used to moderate indoor temperature fluctuations [14]. AHCMs can absorb excess moisture from the air when the indoor RH is higher than a set value (RH_{ad}); or release moisture when the indoor RH is lower than a set value (RH_{des}), precisely maintaining a balanced and comfortable indoor humidity environment without external intervention. In order to achieve the above functionality, AHCM should have the following characteristics. First, the new material needs to have S-shaped (type V [15]) water vapor isotherms (see Fig. 1), showing a steep adsorption curve at the trigger point for adsorption (RH_{ad}), and a steep desorption curve at the trigger point for desorption (RH_{des}). For indoor humidity control, RH_{ad} = 60 %, and RH_{des} = 40 %, because keeping indoor relative humidity levels between 40 % and 60 % can minimize the majority of negative health effects associated with humidity [3] and maximize thermal comfort according to the recommendation of ASHRAE [16]. The RH_{ad} and RH_{des} are tunable depending on the intended applications. Second, the AHCM material should have a large water vapor adsorption capacity at RH_{ad}. Ideally, the maximum water uptake in the targeted control range should be higher than 0.5 g of water vapor per 1 g of dry material. Third, the AHCM should have mild regeneration conditions (i.e., lower regeneration temperature) and highly stable cycling performance. Finally, since AHCM is used for indoor environment control, it must be non-toxic, non-corrosive, and available for large-scale production at a reasonable price.

As mentioned above, most conventional porous sorbents and desiccants cannot meet the requirements for AHCM. Therefore, it is demanded to develop novel sorbent materials that can autonomously regulate indoor humidity, and more efficiently maintain a comfortable and healthy built environment with minimal energy input. Metal-organic frameworks (MOFs), as a recent class of porous materials, have become the focus of research due to their large surface area and pore volume, significant adsorption capacity, and tunable structure and properties [17–19]. The organic-inorganic hybrid character leads to a unique steep stepwise uptake of water vapor [12]. Their strong chemical and structural diversity allows them to tune the hydrophilic/hydrophobic balance easily and is associated in many cases with an easy release at moderate temperatures (50–80 °C) [13] and/or low relative pressures. The regeneration conditions of MOF are influenced by many factors, including the pore size, pore volume, hydrophilicity, as well as the shape of the isotherms. Typically, MOFs with a lower trigger point for steep adsorption require a higher regeneration temperature compared to MOFs with a higher trigger point. Besides, some MOFs have very high working capacities (exceeding 1 g of water vapor per 1 g of MOF in some cases). All these features make MOFs highly attractive and promising as functional materials for energy-efficient applications in the built environment, particularly for humidity control [20–25].

Some pioneering works have been reported in developing/using MOFs as AHCM for automatic humidity control. AbdulHalim et al. have developed a rare-earth-based MOF Y-**shp**-MOF-5 for dual functional moisture control [26]. However, using rare earth elements and the complex synthesis process limit its scale-up production. Abtab et al. have reported a chromium-based MOF with **soc** topology (Cr-**soc**-MOF-1) [27], which can achieve a maximum water uptake of 1.95 g g^{-1} at 70 % RH. However, chromium toxicity hinders its application in indoor environments. Qin et al. have developed a new type of precise humidity control material (PHCM) by using Al/Cr-based MOFs for autonomous humidity control and analyzed its energy impact on building performance in different climates [28]. More recently, some MOFs, such as BIT-66 [29], CAU-1-OH [30], NU-1500-Cr [31], and UiO-67 [32] have been synthesized for moisture control. Although some MOFs have good adsorption performance, only very few of them can meet all criteria for AHCM, especially the requirements concerning safety, cost, and scalability, which are critical for building applications.

This paper reports a novel aluminum MOF-based autonomous humidity control material (MOF-AHCM). The new material has excellent moisture adsorption capacity within the RH range of 40%–60 %. It is highly stable and non-toxic and has the potential for future scale-up by a green synthesis method. Firstly, the synthesis method, physicochemical characterization, and water adsorption (isotherms and moisture buffer value) are investigated. Secondly, laboratory experiments have been carried out to evaluate the moisture control performance of the new MOF-ACHM material under a controlled environment. Finally, the energy impact of using AHCM in different climates is investigated by numerical simulations.

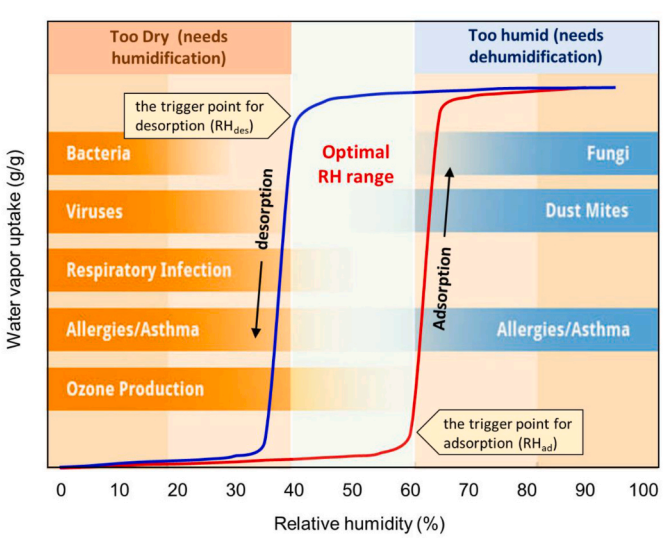

Fig. 1. Water vapor isotherm of idea autonomous humidity control material.

2. Material preparation and characterization

2.1. Synthetic procedures of MOF-AHCM

The new MOF-AHCM prepared in this paper is a muconate analog to Al-MIL-53 [33]. The synthesis route is as follows. 1.65 mmol of $Al_2(SO_4)_3 \bullet 18H_2O$ (Aluminium sulphate octadecahydrate) and 1.65 mmol of trans, *trans*-muconic acid (tt-MA) were ultrasonically mixed in dimethylformamide (DMF) and water solvent solution. The solvent ratio DMF/water is 1:3. The suspension was obtained and then sealed in a 25 mL glass tube. Next, it was placed in a mono-wave microwave reactor with a power of 400 W (Anton Paar GmbH) and heated for 1 h with continuous stirring. After cooling down, the product was separated from the mother liquor and washed 3 times in DMF and then 3 times in water by stirring for about 1 h each time. The new aluminum muconate based MOF-AHCM was obtained by being centrifuged and dried in the air. Finally, the as-synthesized samples were activated in a dynamic vacuum oven by being heated at 120 °C for 12 h. The new MOF-AHCM material was acquired in the form of a grey microcrystalline powder.

2.2. Characterization

2.2.1. Microscopic morphology and chemical characterization

The microscopic morphology and detailed structures of the new MOF-AHCM were investigated using the scanning electron microscope (SEM, Nova NanoSEM). Fig. 2 shows that the micro-crystals of MOF-AHCM have a rectangular rod-like shape with approximately 1 μm in length. Additionally, the powder X-ray diffraction (PXRD) patterns of the synthesized MOF-AHCM were measured with the high-resolution X-ray diffractometer (Rigaku Smartlab). Both the measured and simulated PXRD are presented in Fig. 3. The diffraction peaks of the new MOF-AHCM at 2θ angle values of 9°, 11.2°, and 17.3° well match those simulated from the crystal structure data.

2.2.2. Sorption isotherms

The nitrogen (N_2) ad/desorption isotherms of MOF-AHCM were obtained by ASAP 2020 micromeritics at −196 °C. Three samples (in powder form) were tested. Fig. 4 shows the N_2 sorption isotherms of the synthesized MOF-AHCM. It is a fully reversible IUPAC (type I) isotherm, which demonstrates the permanent microporosity of the new MOF. The porosity parameters of MOF-AHCM were measured and calculated. The Brunauer-Emmett-Teller (BET) specific surface area (S_{BET}) is 1780 m^2g^{-1}, the micropore area ($S_{mirco\text{-}BET}$) is 1580 m^2g^{-1}, the total pore volume ($V_{pore\text{-}total}$) is 0.75 cm^3g^{-1}, and micropore volume ($V_{pore\text{-}micro}$) of the MOF-AHCM is 0.62 cm^3g^{-1}. Fig. 5 shows the pore size distribution calculated from the nitrogen adsorption isotherms using the non-local density functional theory (NLDFT) model. The calculation shows the average pore size of the MOF-AHCM is around 0.9 nm.

Water vapor sorption isotherm is a measure of water content (or water uptake) as a function of relative humidity. The water vapor sorption isotherms of MOF-AHCM were measured by the Dynamic Vapor Sorption (DVS) instrument (DVS Adventure from Surface Measurement Systems, Ltd). Three samples (in powder form) were tested. The water vapor isotherms of the synthesized MOF-AHCM measured at 23 °C are presented in Fig. 6, which shows an IUPAC (type V) S-shaped isotherm. The maximum water uptake is around 0.56 g g^{-1} (at 85 % RH). The steep adsorption starts at around 55 % RH, and the steep desorption begins at approximately 45 % RH, which means the material has the dual functionality of adsorbing water vapor from the indoor environment when the relative humidity is higher than 55 % and desorbing/releasing water vapor to the surroundings when the relative humidity is below 45 %. These features and characteristics meet the basic definition of the autonomous humidity control material for energy-efficient indoor moisture regulation.

The hysteresis of the ad/desorption isotherms falls between 40 % and 70 %. To reveal the relation between adsorbed moisture and relative humidity in the space between the main ad/desorption isotherm curves, the hysteresis scanning isotherms were measured. Fig. 7 shows the scanning desorption isotherms for MOF-AHCM. It's clearly observed that the scanning isotherm curves follow the same shape as the boundary isotherm (or the main isotherm) but are shifted to the corresponding starting point. This indicates MOF-AHCM has a typical H1 hysteresis behavior due to an ordered pore structure [34]. Fig. 8 shows the water uptake of MOF-AHCM during 50 full adsorption-desorption

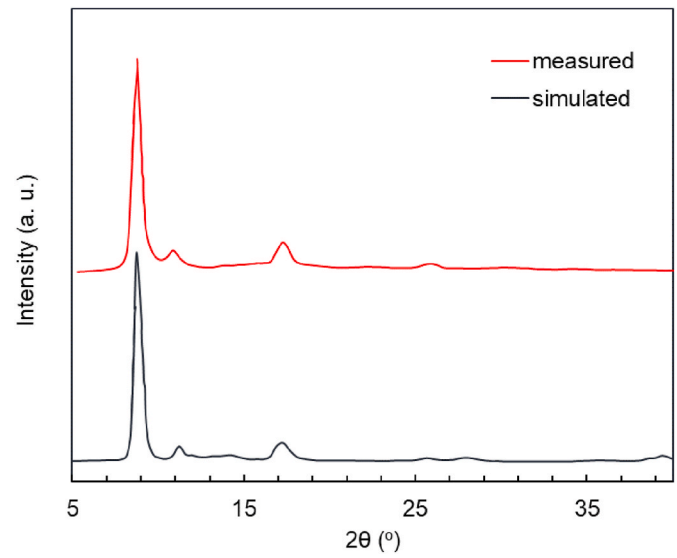

Fig. 3. Powder XRD pattern of MOF-AHCM.

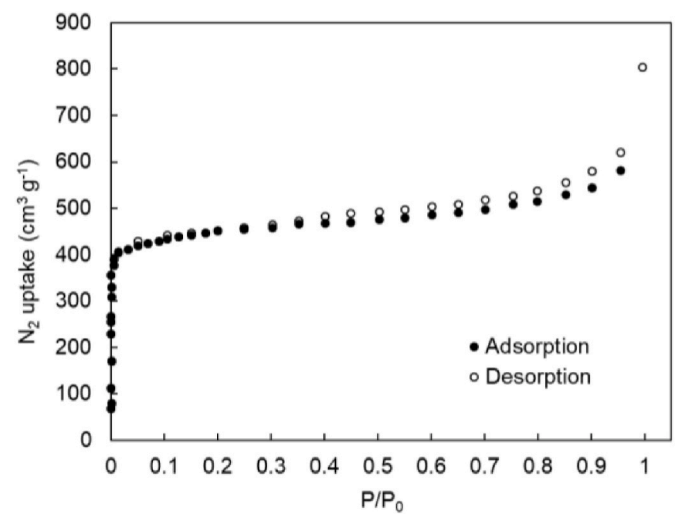

Fig. 4. N_2 ad/desorption isotherms.

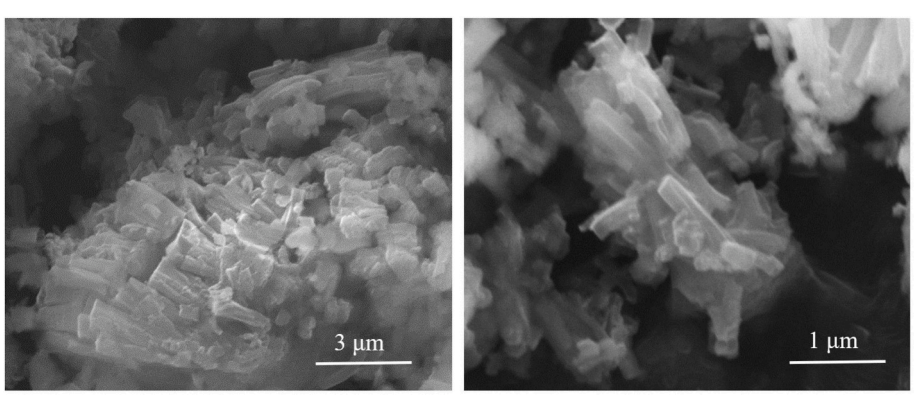

Fig. 2. SEM micrographs of MOF-AHCM.

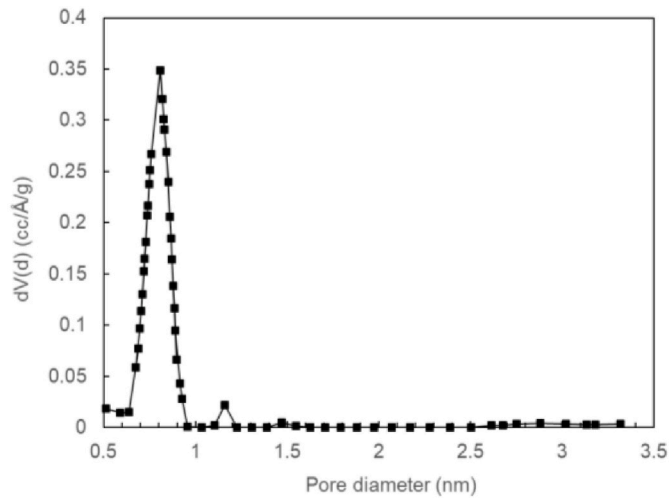

Fig. 5. Pore size distribution analysis.

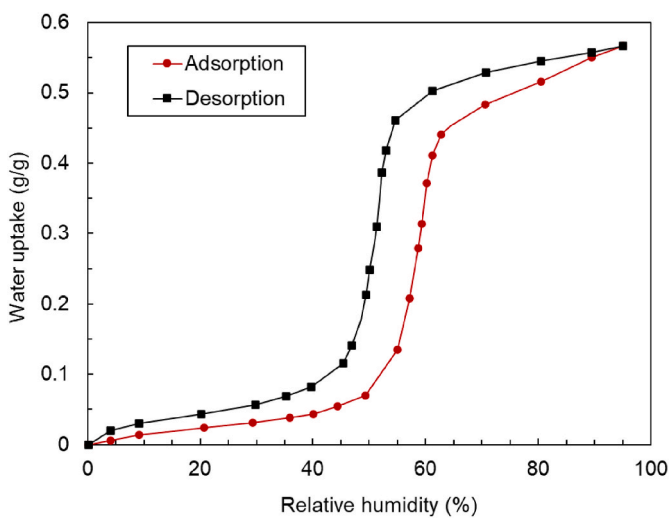

Fig. 6. Water vapor isotherms of MOF-AHCM (Al-MIL-muc).

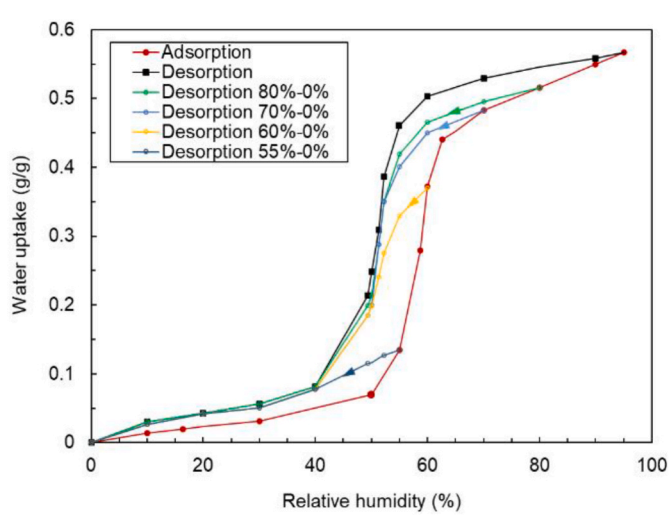

Fig. 7. Hysteresis scanning isotherms of MOF-AHCM.

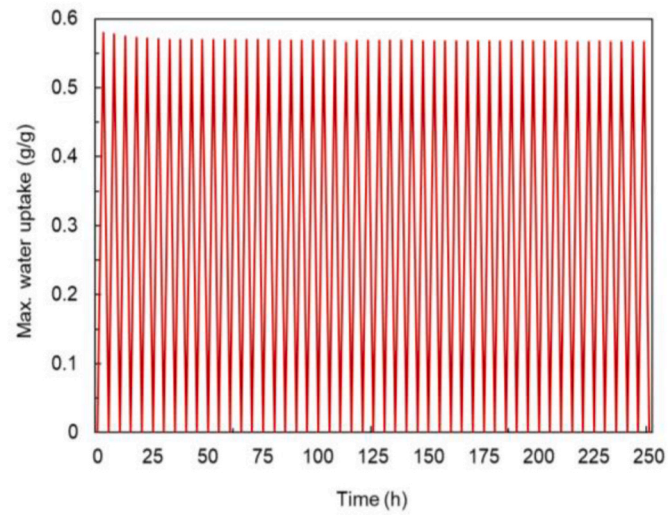

Fig. 8. Water uptake capacity of MOF-AHCM during 50 ad/desorption cycles.

cycles. The results show that there is only a slight (<2 %) decrease in the water uptake capacity during the first 10 cycles, and then the water uptake capacity remains almost constant for the rest of the 40 cycles.

The water sorption isotherms of MOF-AHCM under different temperatures were measured and presented in Fig. 9. It is evident that the hysteresis loop between the adsorption and desorption curves shifts towards the right side of the figure as the temperature increases. Moreover, with rising temperatures, the adsorption capacity exhibits a slight decrease due to the increased hydrophobicity. Nevertheless, the water isotherm shape and adsorption capacity remain almost the same when the temperature is below 40 °C. Since the indoor temperature rarely exceeds 40 °C, the new MOF-AHCM works efficiently in most building applications.

Fig. 10 shows the comparison of the water sorption isotherms of different MOFs and representative hygroscopic building materials. The results indicate: (1) the water uptake of MOFs is much higher than that of conventional hygroscopic building materials (e.g., spruce board and gypsum); (2) only MOF-AHCM (Al-MIL-muc) meets the criteria of autonomous humidity control materials with S-shape isotherm between 40 % and 65 % RH.

The heat of adsorption of the synthesized MOF-AHCM was measured using a micro-calorimeter. The average heat of adsorption is approximately 48 kJ mol^{-1}, about 17 % above the evaporation enthalpy of water (41 kJ mol^{-1}). The isosteric heat of water adsorption $\Delta H_{ads}(H_2O)$

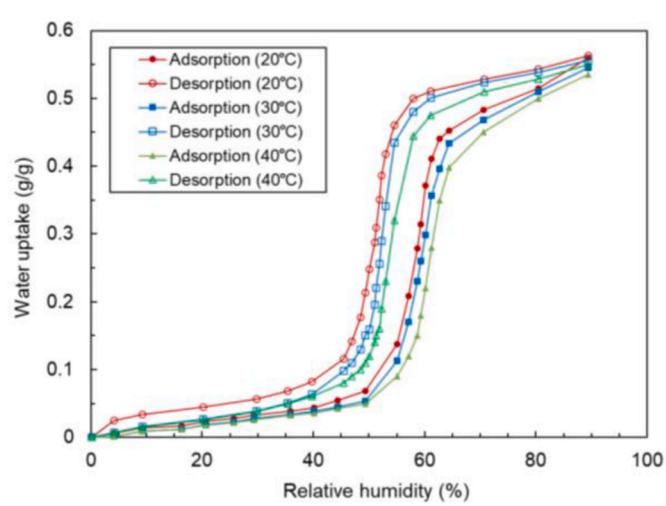

Fig. 9. Water vapor isotherms of MOF-AHCM under different temperatures.

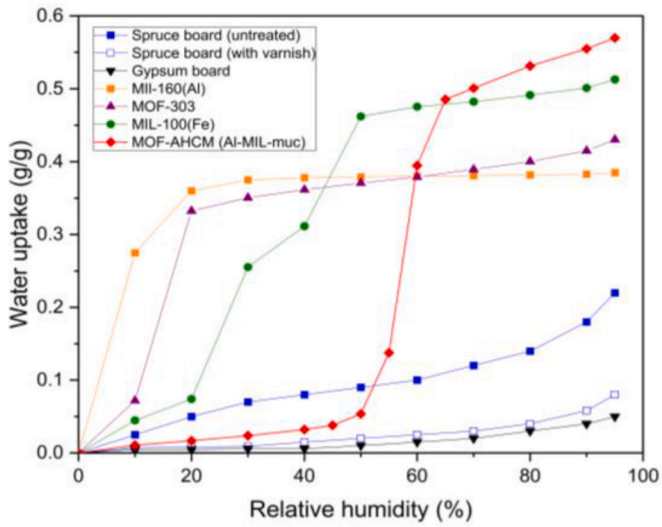

Fig. 10. Comparison of water vapor adsorption isotherms of different hygroscopic materials.

was also calculated by applying the Clausius–Clapeyron equation from water adsorption isotherms collected at 20, 30, and 40 °C, respectively. The calculation shows an average value of 47–50 kJ mol^{-1}, which fits the experimental data quite well.

2.2.3. Moisture buffer value

Moisture buffering refers to the capacity of materials to mitigate fluctuations in relative humidity by absorbing or releasing water vapor from the ambient air. Hygroscopic porous materials with large moisture buffering ability can significantly impact indoor humidity conditions and building energy performance [35]. To assess the moisture buffering ability of various porous materials, Rode et al. [36] introduced the notion of moisture buffer value (MBV). This metric gauges the quantity of water vapor that a material uptakes or releases when subjected to fluctuating relative humidity between two defined levels during a day (24 h). As outlined in the NORDTEST test protocol [36], MBV quantifies the vapor adsorption or desorption by hygroscopic materials in response to a square wave pattern of humidity shifts (e.g., 8 h of 75 % high RH followed by 16 h of 33 % low RH). Recently, enhancements to the MBV theory and testing techniques were put forth by Qin et al. [37,38].

In this study, the MBV of the newly synthesized MOF-AHCM was measured in the building physics lab at the Technical University of Denmark (DTU) according to the NORDTEST test protocol. The experimental setup is shown in Fig. 11, which mainly consists of a climatic chamber and an automated weighing system. The climatic chamber maintained a uniform temperature of 23 ± 0.2 °C. Temperature sensors (accuracy of ±0.2 °C) and humidity sensors (accuracy of ±1 %) fed information to a proportional integral derivative (P.I.D.) controller and computer system. The chamber's internal humidity level remained stable (±1 % RH) through a controlled mixing of saturated and dry air proportions by the P.I.D. controller. Internal climate uniformity was maintained by a small axial fan. A humidity cycle (i.e., a day) of 8 h at a high RH level (75 %) followed by 16 h at a low RH level (33 %) was initiated within the chamber, with swift humidity transitions. The weight of the test samples was measured and recorded automatically by the weight system (accuracy of ±0.001 g) every 5 min.

The samples were fully activated at 100 °C for 12 h before the test. The activated MOF-AHCM was placed in a petri dish with a diameter of 60 ± 0.5 mm. The thickness of the sample is 15 ± 0.5 mm. Only the top surface of the sample was exposed to the air with cyclic RH changes air in the climatic chamber. The test was carried out through multiple cycles to attain a relatively stable MBV for the samples. The MBV was obtained by calculating the water vapor uptake/release per open surface area (m^2) per relative humidity variation (%) during a cycle of the ad/

Table 1
Comparison of the MBVs of different porous materials.

Materials		MBV ($g \cdot m^{-2} \cdot RH^{-1}$)	Ref.
MOFs	MOF-AHCM	12.08 ± 0.12	This work
	MIL-100(Fe)	5.17 ± 0.15	[39]
	MOF-303	4.82 ± 0.09	[39]
	Al fum	2.29 ± 0.08	[39]
	MIL-160(Al)	1.08 ± 0.07	[39]
Conventional hygroscopic materials	Spruce board (untreated)	1.22 ± 0.04	This work
	Spruce board (with varnish)	0.55 ± 0.08	This work
	Cellular concrete	1.05 ± 0.07	[36]
	Vesuvianite	0.79 ± 0.12	[40]
	Gypsum	0.57 ± 0.13	[36]
	Sepiolite	0.54 ± 0.15	[40]
	Laminated Wood	0.46 ± 0.07	[36]
	Brick	0.39 ± 0.11	[36]
	Concrete	0.37 ± 0.11	[36]

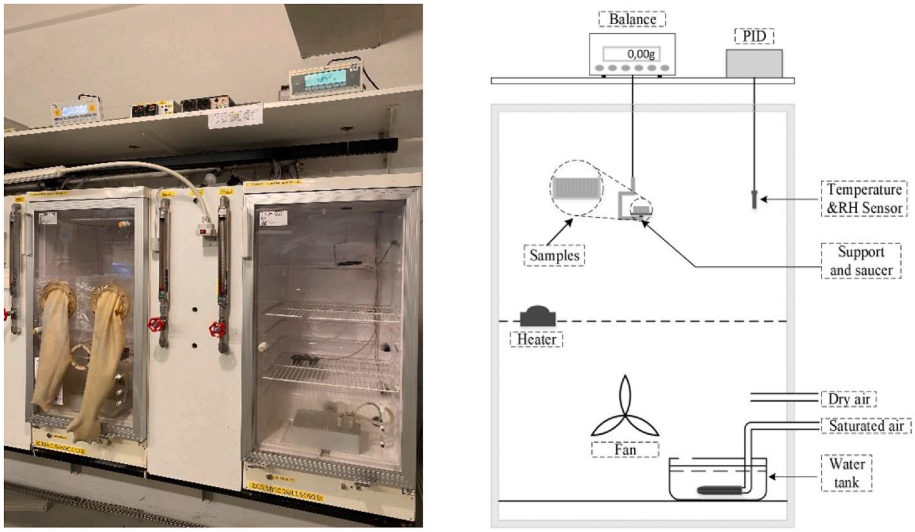

Fig. 11. The experimental setup for the MBV test.

desorption process. Three samples were tested for each material and the mean MBV was determined by averaging three measurements. The uncertainties associated with the MBV results were further elaborated in Table 1. The MBV of MOF-AHCM is 12.08 ± 0.12 g m^{-2}·RH^{-1}, which surpasses that of most conventional construction materials by a significant factor and also outperforms other MOF-based desiccants, such as MIL-100(Fe), MIL-160(Al), and MOF-303 et al. [39] (see the comparison in Table 1). The test results prove that the novel AHCM boasts remarkable moisture buffering capabilities within the hygroscopic region, which positions the new material as an up-and-coming candidate for an optimal moisture adsorbent for regulating indoor relative humidity.

2.2.4. Stabilities and cyclabilities

Hydrothermal stability is one of the basic prerequisites for utilizing an adsorbent in a built environment. The DVS tests under different temperatures (Fig. 9) confirm that MOF-AHCM has a good adsorption capacity in most temperature conditions in buildings. Thermogravimetric analysis (TGA) was conducted to study the thermal stability of the new MOF-AHCM under high-temperature conditions. Fig. 12 shows the TGA analysis performed in air, which unveils the robust thermal resilience of MOF-AHCM, demonstrating its ability to endure high temperatures reaching up to 400 °C. The test outcomes illustrate the versatility of the new MOF-AHCM, showcasing its potential not only in autonomous indoor humidity regulation but also in applications related to adsorption chillers and heat pumps. Furthermore, stability tests involving multiple ad/desorption cycles were conducted. The test outcomes reveal that the water vapor adsorption capacity of the new MOF-AHCM remains consistent after undergoing 50 consecutive cycles of water adsorption and desorption (see Fig. 8). These test results confirm that the new MOF-AHCM is a stable material for practical application in buildings.

2.2.5. Safety, cost, and scalability

The toxicity of MOFs is one of the most important concerns, as these materials may be harmful to human health in direct contact. The selection of green materials should be of high priority for indoor applications. The developed MOF-AHCM (Al-MIL-muc) is an aluminum-based MOF. Al is regarded as one of the green transition metals and is safe for indoor applications [21]. However, many MOFs from previous studies for automatic humidity control, such as Cr-**soc**-MOF-1 [27], NU-1500-Cr [31], and Y-shp-MOF-5 [26], etc., are either chromium-based or rare-earth-based MOFs. Those metal ions have certain toxicity and are not suitable for direct indoor applications.

Regarding cost and scalability, MOFs are an emerging class of new porous material. MOFs' commercialization has started, but large-scale industrial production has not yet taken place. It is difficult to directly compare the market prices of different MOFs. However, we can make a simple estimation by comparing the cost of the raw materials (i.e., metal ions and ligands). Some researchers have conducted a complete assessment of the MOF production costs, and predict that the expected cost of some aluminum-based MOFs ranged from about 55 $ per kg at 100 tons per year down to 29.5 $ per kg for 1 kton per year production with longer-term perspectives of reaching costs below 10 $ per kg once the bio-derived ligand is considered for the large-scale production [41]. The costs of Cr-based and rare-earth-based MOFs are one magnitude higher than Al-based MOFs.

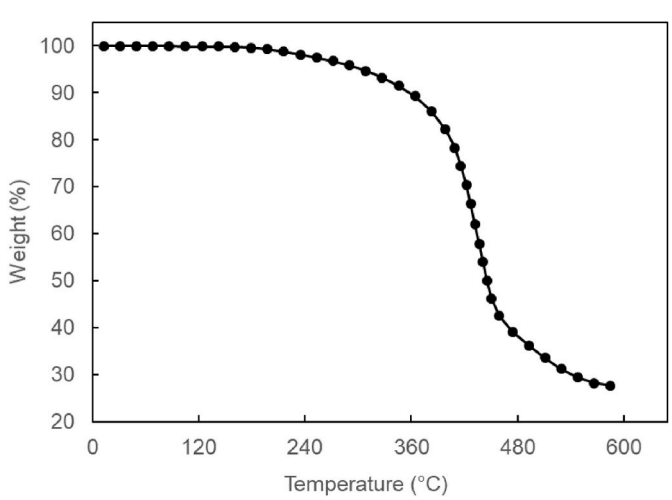

Fig. 12. TGA curves of MOF-AHCM.

3. Moisture control performance of MOF-AHCM

3.1. Experimental test

3.1.1. The test room

The material characterizations in Section 2 indicate that the new MOF-AHCM has excellent moisture adsorption abilities. To verify its humidity control performance in the real built environment, experimental tests were carried out in the full-scale test cell at DTU. Fig. 13 shows the external view of the test cell. It's a steel structure with a very high airtightness and insulation. The walls are insulated with 0.50 m of polystyrene and mineral wool and are covered with steel sheets on both the inside and the outside. The air change rate (ACR) of the test cell has been measured with tracer gas using the decay method and found to be about 0.20 h^{-1} at 50 Pa (0.015 in Hg) pressure difference. Without pressurization, the ACR was about 0.007 h^{-1}. The floor area of the test room used in this study is 8 m^2, and the ceiling height is 2.5 m. The interior surfaces of all walls, ceilings, and floors are coated with polyethylene foil to create a vapor-tight and non-absorbing barrier. The test room is equipped with high-precision sensors to measure outdoor climate and indoor hygrothermal conditions, including air temperatures and relative humidity. Fig. 14 shows the schematic of the internal structure of the test cell.

A humidity control apparatus (shown in Fig. 15) was installed in the test room, which can generate/remove a given amount of water vapor to/from the indoor air. Through the control system of the apparatus, it becomes feasible to manage the rates of evaporation and condensation according to a predefined timetable. This controlled evaporation of water mimics the moisture generation in an occupied room, while controlled condensation is employed to simulate the removal of moisture from the room, typically through ventilation in residential buildings. The detailed design and test of the humidity control apparatus can be found in Ref. [42]. Two fans were installed in the test room to ensure the air was well-mixed during the experiments.

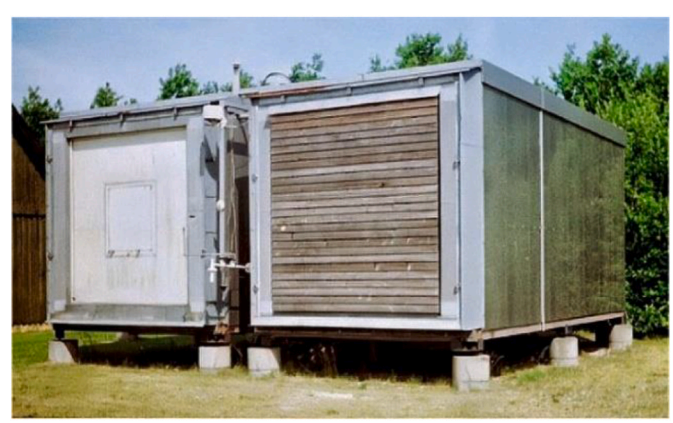

Fig. 13. Exterior view of the test cells at DTU.

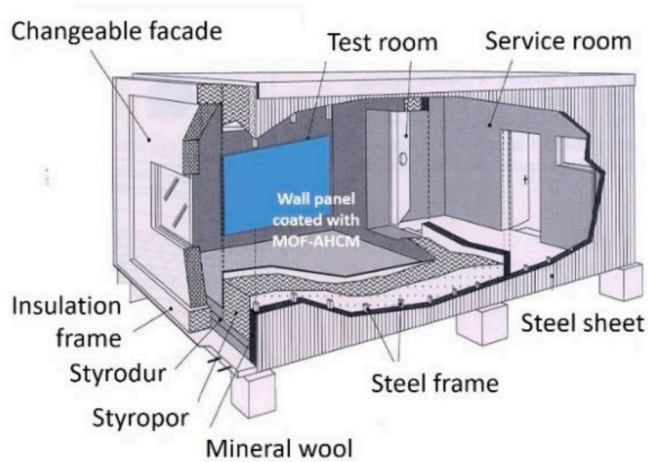

Fig. 14. Schematic of the internal structure of the test cell.

3.1.2. Measurements

The experimental measurements were conducted within the test chamber outlined in the preceding section. The primary objective of these measurements was to gather data regarding the moisture buffering capacity of the newly synthesized MOF-AHCM materials. The moisture buffering performance of the plasterboard was also measured as a comparison. The reasons for choosing plasterboard for comparison are as follows: First, plasterboard is one of the most widely used building materials for creating interior walls and ceilings in residential buildings. Its moisture buffering performance has been studied by many researchers [43]. Plasterboard is often chosen as the benchmark material for comparing moisture buffer capacities. Second, although the MBV of the untreated spruce board listed in Table 1 is higher than that of gypsum, untreated spruce wood is rarely directly used for indoor furnishing due to durability issues. In most cases, spruce wood is treated with oil, wax, or varnish. The MBV of the spruce board with varnish is similar to the MBV of gypsum. Therefore, plasterboards were used for comparison with the new MOF-AHCM.

Three experimental series have been carried out. The detailed descriptions are listed in Table 2. The indoor temperature was controlled at 20 ± 0.5 °C during the experiments. The humidity control apparatus first worked as a humidifier that injected 240 ± 0.1 g of water vapor into the indoor air at a constant rate for 12 h and then switched to a dehumidifier that removed 240 ± 0.1 g of water vapor from the indoor air by condensation for the following 12 h. Each measurement was conducted for several days until a stable daily cycle was achieved. The results of the last daily cycle were used for analysis.

3.1.3. Test results

The measured indoor relative humidity variations of the empty chamber (Case I) are presented in Fig. 16. The predicted indoor relative humidity was calculated from the actual amount of water vapor that the humidity control apparatus injected into the chamber. The slight discrepancy between the measured and predicted curves is probably due to the air leakage of the chamber and the water vapor adsorption/condensation on the internal surfaces, especially at high RH conditions. The inaccuracies in the calibration and measurement of the different

Table 2
Descriptions of the experimental series.

Case	Descriptions
Case I (empty chamber)	The chamber is completely empty; all internal surfaces are covered by polyethylene foil; no moisture transfer from/to the internal surfaces; no ventilation; and highly airtight. This is a reference case.
Case II (MOF-AHCM panel)	A wall panel (2 m × 1.5 m) coated with MOF-AHCM was hung on the wall in the empty chamber; the thickness of the MOF coating is 3 mm; there is no other moisture sorbent in the room; no ventilation, and highly airtight.
Case III (plasterboard)	A piece of plasterboard (2 m × 1.5 m) was installed on the wall in the empty chamber; the thickness of the plasterboard is 15 mm; there is no other moisture sorbent in the room, no ventilation, and highly airtight.

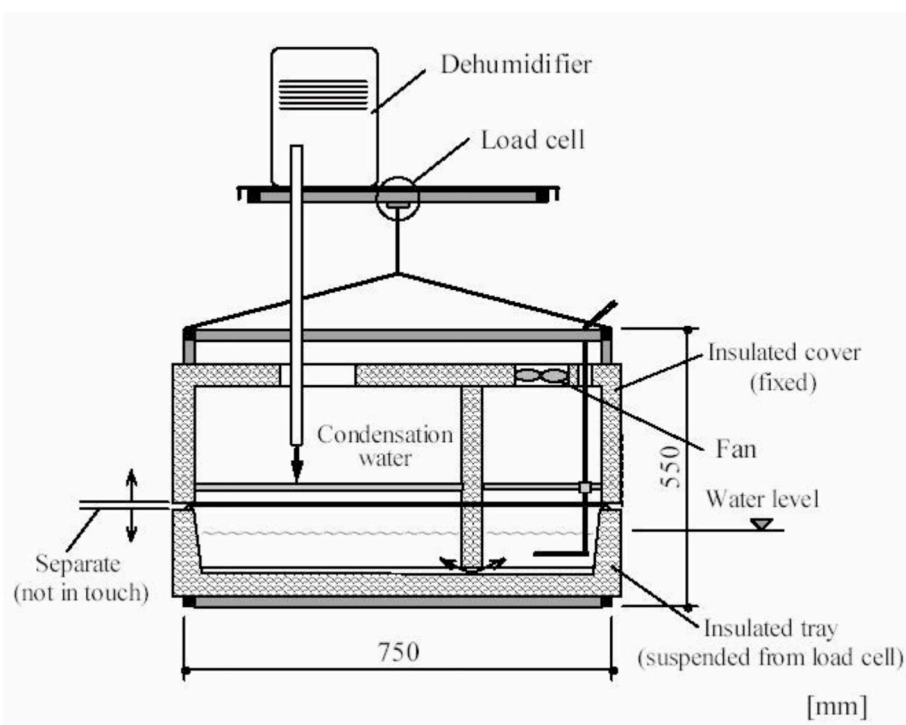

Fig. 15. Schematic of the humidity control apparatus [42].

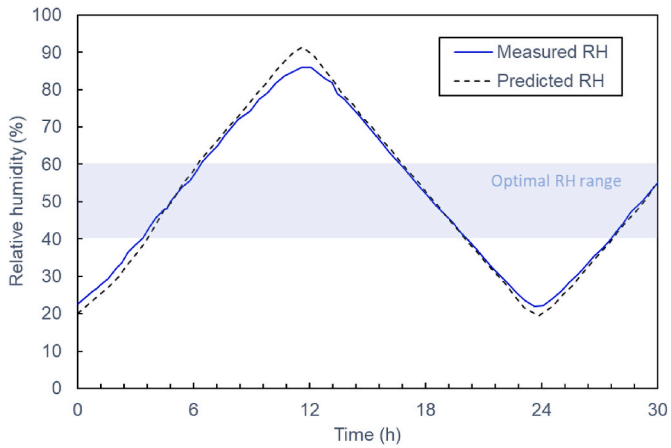

Fig. 16. The variations of relative humidity in the empty chamber (Case I).

sensors might also be a minor issue. Nevertheless, Fig. 16 illustrates that the humidity control apparatus can effectively manage the rates of water evaporation and condensation, ensuring that the indoor relative humidity fluctuations align with a predefined schedule. Case I (empty chamber) is the reference for the following tests. Different moisture buffering materials were added to the chamber for Cases II and III testing.

Fig. 17 illustrates variations in indoor relative humidity achieved through the utilization of different moisture buffering materials, specifically, a MOF-AHCM panel (case II) and a plasterboard (case III). In case II, the MOF-AHCM panel effectively mitigates indoor moisture fluctuations, maintaining indoor relative humidity within the designated range of 40 %–60 %. This implies that no supplementary humidity control is necessary. The experimental results demonstrate that the new MOF-AHCM material can autonomously maintain the indoor relative humidity within the thermal comfort range without requiring additional energy input.

Conversely, the test results for case III reveal that the plasterboard also possesses some degree of moisture buffering capacity. However, indoor relative humidity fluctuations within case III (ranging between 31 % and 72 %) are notably more pronounced than those observed in case II. Throughout 55 % time of the day, indoor relative humidity in case III falls outside the recommended range of 40 %–60 % RH. This suggests a potential need for supplementary dehumidification or humidification, which may cause additional energy consumption. Consequently, the plasterboard falls short of achieving autonomous indoor humidity control.

Furthermore, the tests also demonstrate that the MOF-AHCM has a fast ad/desorption response to indoor relative humidity changes, which is another advantage over many conventional desiccants (e.g., silica gel and hydrogel, etc.) and common hygroscopic materials (e.g., wood, plasterboard, etc.) in the built environment. To sum up, the investigation reveals several critical merits of the newly synthesized aluminum muconate-based MOF-AHCM: large adsorption capacity, fast kinetics, mild regeneration requirements, stability, and safety. Furthermore, its potential for eco-friendly large-scale synthesis adds to its appeal. Altogether, these characteristics position it as a promising candidate for achieving autonomous humidity control in the built environment.

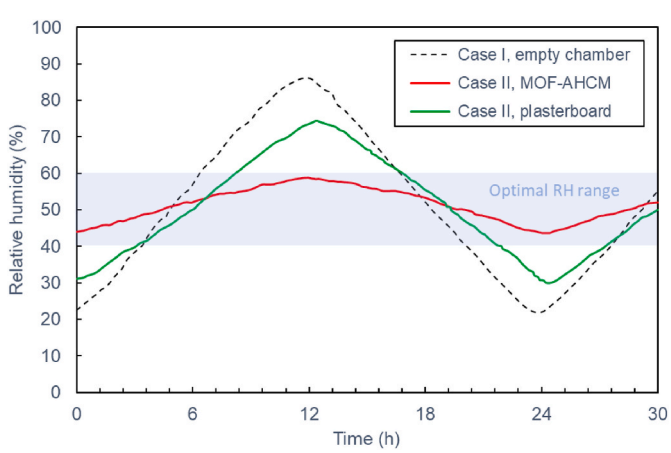

Fig. 17. Indoor relative humidity variations of Case II and Case III.

3.2. Simulation of energy saving potential

The materials characterization and full-scale chamber tests in previous sections collectively reveal that the synthesized MOF-AHCM has an exceptional moisture control ability. In this section, further investigation of the impact of MOF-AHCM on building energy consumption will be carried out by numerical simulation. Moreover, the energy-saving potential of using MOF-AHCM in buildings in climates with different moisture types worldwide will be analyzed.

3.2.1. Numerical model

The scientific program used for the simulation is MATCH/BSim. MATCH/BSim, a holistic model based on the coupled heat, air, and moisture (HAM) calculation model, was initially developed at the Technical University of Denmark (DTU) [44,45]. This model considers water vapor diffusion, vapor ad/desorption, liquid water transport, sources and sinks of moisture inside a component, and thermal parameters. It has been widely used in building hygrothermal analysis.

The following assumptions and limitations are considered in the MATCH hygrothermal building simulation: (1) the air temperature is constant within each zone: Temperature and humidity are the same throughout the room, and the air is thoroughly mixed. (2) Heat and moisture transfer processes through components are considered to be one-dimensional. Consequently, the entire surface of each component has a constant temperature. (3) Physical material properties are not time-dependent.

In the MATCH/BSim model, the moisture balance equation in the room air is defined as:

$$\frac{dm_i}{dt} = \sum_j C_{constr,j} + C_s + C_{Vent} + C_{HVAC} \tag{1}$$

Where, m_i is the overall moisture content of the air in the ith zone [kg]; t is the time [s]; $C_{constr,j}$ is the moisture flow between the inner wall surface j and room air [kg]; C_s is the moisture source in the room [kg s^{-1}]; C_{Vent} is the moisture flow due to ventilation [kg s^{-1}]; C_{HVAC} is the moisture flow due to the HVAC systems [kg s^{-1}].

The moisture flow between the inner wall and room air can be calculated from:

$$C_{constr} = A_{surf} * \beta * \left(p_{surf} - p_{air}\right) \tag{2}$$

Where A_{surf} is the surface area [m^2]; β is the water vapor transfer coefficient [kg m^{-2}s^{-1}Pa^{-1}]; p_{air} is the partial water vapor pressure in the zone [Pa]; p_{surf} is the partial water vapor pressure on the component surface [Pa].

The moisture transfer within the building material/envelope between the interior and exterior walls is calculated by a finite control volume method. The model mainly considers vapor diffusion across the building envelope, as well as the vapor ad/desorption at the interior wall surfaces. The model also takes into account the temperature impact on moisture transport [46]. MATCH/BSim are widely utilized for moisture simulation in buildings [44,45]. These software tools have undergone rigorous validation through a series of studies [46]. The MATCH software is particularly notable for its incorporation of moisture hysteresis

between adsorption and desorption isotherm curves [47] - a critical consideration for materials displaying substantial moisture hysteresis, as seen in the case of MOF-AHCM.

3.2.2. Moisture climates

The effectiveness of autonomous humidity control materials is significantly influenced by outdoor moisture conditions. To investigate the performance of MOF-AHCM in different moisture climates, 10 cities with varying conditions of moisture worldwide are selected according to the revised Thornthwaite-type global climate classification of moisture variation [48]. Fig. S1 (in the appendix) shows the Thornthwaite global distribution of moisture variation. It consists of 6 different moisture types, including 3 humid regimes (i.e., Moist, Wet, and Saturated) and 3 dry regimes (i.e., Arid, Semiarid, and Dry). The Thornthwaite moisture classification is based on the moisture index value [48]. In this study, two representative cities from each moisture type have been selected for the simulation research, except the saturated area as they are typically only found in the polar regions. Detailed information on the selected cities is listed in Table S1 (in the appendix).

3.2.3. Test room and simulation cases

The test room used in the experimental tests was adopted for the simulation studies. It was presumed to be an office space, utilized from 9:00 a.m. to 5:00 p.m. During the occupied period, there is one person working in the office. The average energy output of an adult working in an office is 120 W. Therefore, the internal heat load 15 W m^{-2}. The person will also generate 100 g of water vapor per hour. Therefore, the internal humidity load is 5 g $m^{-3}h^{-1}$.

There is a temperature and humidity independent control system (THIC) [49] in the office. The sensible cooling load and latent cooling load are handled separately by different units. The latent load will be handled by a desiccant system. The THIC system can maximize the advantage of using MOF-AHCM materials. The room temperature is maintained at 26 °C, and the allowable indoor relative humidity range is between 40 % and 65 % during the occupied period. According to the ASHRAE standard 62.1, the minimum ventilation rate for outdoor air in office spaces is 2.5 L/(s•person) [50]. In this study, the air change rate is 0.5 h^{-1} during the occupied period and 1 h^{-1} during the unoccupied period. The ventilation during the unoccupied period is to regenerate the MOF-AHCM using outdoor air at night. There is no temperature and humidity control during the unoccupied period.

There are three simulation cases for each city/climate. They are:

Case S.I - There is no moisture buffer material inside the office; all internal surfaces are assumed covered by polyethylene foil. This is a reference case.

Case S.II - There are two wall panels (2 m × 1.5 m) coated with MOF-AHCM hung on the wall in the office; The thickness of the MOF coating is 3 mm. The substrate is hydrophobic and there is no other moisture sorbent in the room.

Case S.III - Two pieces of plasterboard (2 m × 1.5 m) are installed on the wall in the empty chamber. The thickness of the plasterboard is 15 mm.

3.2.4. Results and discussion

As the moisture buffering phenomenon of hygroscopic materials mainly influences indoor humidity fluctuations, its impact on indoor temperature can be negligible [20,38,51,52]. The primary emphasis of the simulation study presented in this paper is on moisture transfer and the latent cooling load of the office. The simulated energy-saving rates of latent cooling load using MOF-AHCM in different cities/climates are presented in Fig. 18. The detailed calculated results are summarized in Table 3.

The simulation reveals that MOF-AHCM can autonomously handle all latent cooling loads in arid and semi-arid climates and regulate the indoor humidity level within the thermal comfort range. The MOF-AHCM will adsorb moisture when the indoor relative humidity is higher than the set value (i.e. 60 % RH) during the occupied period; and can be fully regenerated (release moisture) by the dry air from outside through nighttime ventilation during the un-occupied period. The moisture adsorption and desorption can be completed within a daily cycle at most times of the year. Additional humidity control processes are unnecessary in the HVAC systems in these climates.

For dry climates, the MOF-AHCM panel demonstrates the capability to manage 75%–86 % of the latent cooling load. This implies that indoor relative humidity levels remain within the thermal comfort range for the majority of the year, although occasional exceedances of 65 % RH occur on a few days. A more comprehensive analysis of indoor relative humidity during these periods revealed that indoor RH levels seldom surpassed the threshold of 70 %. Despite residing slightly above the thermal comfort range, indoor humidity levels remain within the acceptable upper limits, and only a few days of elevated humidity pose no threat of mold or health concerns. Consequently, in the summertime of dry climates (e.g., Madrid and Lanzhou), there's generally no need for dehumidification when employing MOF-AHCM. This is particularly pertinent as the evening's average outdoor humidity often falls below

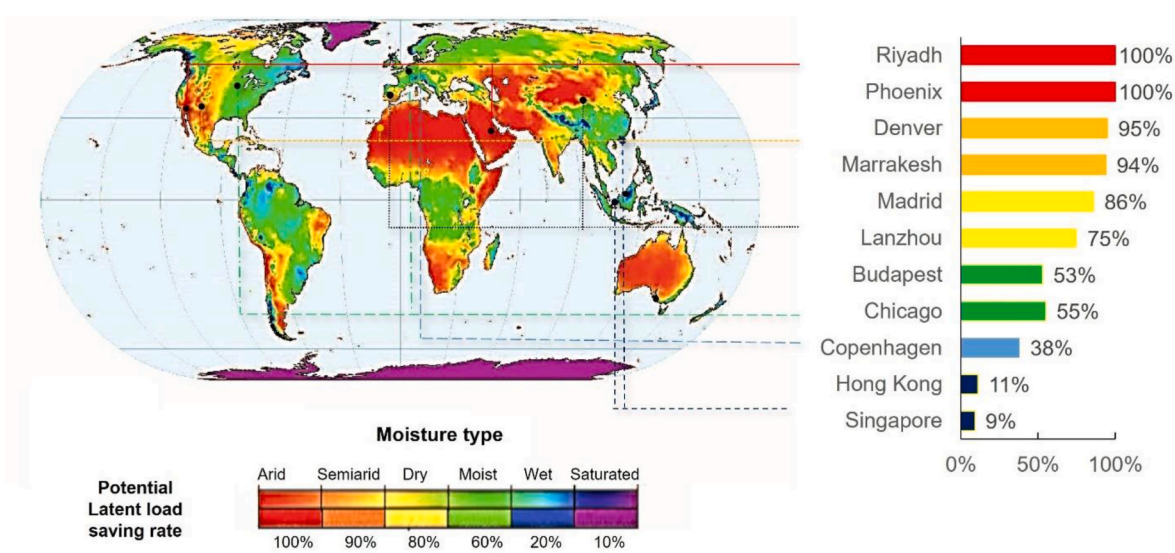

Fig. 18. Simulated energy-saving rate of latent cooling load by using MOF-AHCM in different cities/climates.

Table 3
Simulated latent cooling load by using MOF-AHCM and plasterboard in different moisture climates/cities.

City/Moisture type	Case	Latent cooling load (W·m^{-2})	Latent cooling load removed by moisture buffer materials (W·m^{-2})	Energy-saving rate of latent cooling load (%)
Riyadh, Saudi Arabia /Arid	Case S.I	5.9	–	–
	Case S.II	0	5.9	100 %
	Case S.III	2.4	3.5	59 %
Phoenix, USA /Arid	Case S.I	7.3	–	–
	Case S.II	0	7.3	100 %
	Case S.III	3.7	3.6	49 %
Denver, USA /Semi-arid	Case S.I	8.6	–	–
	Case S.II	0.3	8.3	95 %
	Case S.III	5.0	3.6	42 %
Marrakesh, Morocco /Semi-arid	Case S.I	9.6	–	–
	Case S.II	0.6	9.0	94 %
	Case S.III	6.3	3.3	35 %
Madrid, Spain /Dry	Case S.I	11.2	–	–
	Case S.II	1.6	9.6	86 %
	Case S.III	8.2	3.0	27 %
Lanzhou, China /Dry	Case S.I	11.8	–	–
	Case S.II	2.9	8.9	75 %
	Case S.III	8.9	2.9	25 %
Budapest, Hungary /Moist	Case S.I	15.3	–	–
	Case S.II	7.2	8.1	53 %
	Case S.III	13.2	2.1	13 %
Chicago, USA /Moist	Case S.I	17.3	–	–
	Case S.II	7.8	9.5	55 %
	Case S.III	15.2	2.1	12 %
Copenhagen, Denmark /Moist	Case S.I	18.6	–	–
	Case S.II	11.5	7.1	38 %
	Case S.III	17.9	0.69	8 %
Hong Kong, China /Wet	Case S.II	27.2	–	–
	Case S.III	24.2	3.0	11 %
	Case S.III	26.7	0.5	2 %
Singapore, Singapore /Wet	Case S.I	28.5	–	–
	Case S.II	25.9	2.6	9 %
	Case S.III	27.6	0.9	3 %

40 % RH, allowing MOF-AHCM to be efficiently regenerated through nighttime ventilation with dry outdoor air. However, it's imperative to discontinue nighttime ventilation once most of the MOF materials have undergone successful regeneration to prevent material re-absorption of moisture in the evening. With well-designed ventilation control strategies, MOF-AHCM can also autonomously modulate indoor air humidity conditions in dry climates.

For moist climates (e.g., Budapest and Chicago), the simulated results show that the energy-saving rate of latent cooling load in the case with MOF-AHCM is around 55 %. This rate is notably lower compared to arid, semiarid, and dry climates. The primary rationale behind this disparity resides in the higher atmospheric humidity observed during evening hours (the unoccupied period) in Budapest and Chicago, as opposed to the drier conditions in the three previously discussed climates. Consequently, the complete regeneration of MOF-AHCM through nighttime ventilation is unattainable. The statistical analysis demonstrates that the evening outdoor humidity levels meet the prerequisites for MOF regeneration during approximately half of the summer days. Conversely, this implies that MOF-AHCM cannot achieve complete regeneration during the remaining half of summer days. Should MOF-AHCM fail to regenerate during the evening, its moisture buffering capacity will be substantially compromised on the subsequent day. In such instances, supplementary dehumidification might be needed to control the indoor humidity level within the acceptable range. Nevertheless, the utilization of MOF-AHCM still enables passive savings of approximately 55 % in latent cooling load in moist climates.

In wet climates (e.g., Hong Kong and Singapore), the diurnal outdoor relative humidity remains consistently high. Variations in daily temperature and humidity levels are small. Throughout the majority of the summer season, outdoor humidity levels exceed the desorption thresholds for MOFs, exerting a notable influence on the efficacy of MOF-AHCM. Once MOF-AHCM reaches saturation, passive methods, such as nighttime ventilation, prove insufficient for complete desiccation of the wet MOF-AHCM, posing significant challenges in this regard. The simulated energy-saving rate for the cases with MOF-AHCM is around 10 %, which indicates MOF-AHCM exhibits limitations in achieving optimal functionality through exclusively passive means in wet climates.

However, this does not imply that MOF-AHCM materials cannot be utilized in wet climates. When combined with an appropriate regeneration system, the new MOF-AHCM materials can still effectively regulate indoor humidity autonomously. Typically, MOF materials can be fully regenerated through either desiccation with dry air (air RH is lower than the desorption RH), or through thermal heating processes. It is worth noting that, in comparison to conventional sorbents/desiccants (e.g., zeolite, silica gel, etc. [53,54]), some MOFs (e.g., the as-synthesized MOF-AHCM) and their related composites exhibit significantly lower regeneration temperatures (around 50–70 °C) [55,56]. This is one of the main advantages of MOF-based sorbents, and this characteristic enables the potential utilization of low-grade energy sources, such as solar energy or waste heat from thermal power plants, to dry the saturated MOF materials.

For the regeneration of MOF-AHCM in wet/humid climates, there are two simple methods. (1) Solar thermal regeneration: This method entails the utilization of direct solar irradiation. The MOF-AHCM material is subjected to direct exposure to sunlight, and as the surface temperature surpasses the threshold of 50 °C, the regeneration process is initiated. This can be accomplished in about 30 min. In order to maintain a continuous operation, two MOF-PHCM panels are needed. One is in use and the other one is under regeneration by natural sunlight, and switch them every day at the beginning of the occupied period. (2) Integration with renewable energy-based heating: The second approach involves the incorporation of a heating element/system powered by renewable energy sources, such as integrating the MOF-PHCM wall panel with a heater (e.g., coat the MOFs on the surface of a panel heater), and then maintain the surface temperature around 50–60 °C for 20–30 min [4]. Once the MOF-AHCM material has regenerated through either of these

techniques, it can be promptly reemployed for humidity management, enabling autonomous indoor moisture control in wet climates. However, detailed descriptions of the MOF-AHCM heating regeneration system are beyond the scope of this study. We plan to share these details in future publications.

Besides, it's worth noting that, as seen in Fig. 18, wet climates occupy only a small fraction of the globe, primarily concentrated near the equatorial regions of Southeast Asia and South America. This indicates that MOF materials can be used effectively to control indoor humidity in many regions worldwide in a purely passive manner.

The energy-saving potentials of using plasterboard in different cities and climates were also calculated, and shown in Table 3. The simulation results indicate that the plasterboard also possesses some moisture buffering capacity, but its energy-saving potential is significantly lower compared to the MOF-AHCM panel. Moreover, in moist and wet climates, the energy-saving potential of using plasterboard can be considered negligible. It is worth mentioning that the exposure area for both MOF-AHCM and plasterboard is identical, however, the thicknesses are different. We only use a 3 mm coating for MOF-AHCM, while the thickness of the plasterboard used in the study is 15 mm. Considering the densities of both materials ($\rho_{MOF} = 380$ kg m^{-3}, $\rho_{gypsum} = 980$ kg m^{-3}), the total weight of MOF-AHCM used in the study is merely 6.85 kg, compared to the plasterboard's weight of 88.2 kg. This explains why plasterboard also exhibits some energy-saving potential in some climates despite its significantly lower moisture adsorption capacity compared to MOFs. It is because its mass is more than 12 times higher than that of MOF-AHCM. The total moisture absorbed by a material equals its water uptake (per gram of dry material) multiplied by the material's total mass. If using the same amount of gypsum as MOFs, the energy-saving potential of plasterboard is almost negligible in most climates. This also indicates the exceptional moisture adsorption capacity of MOF-AHCM.

4. Conclusion

In this paper, a novel MOF-based autonomous humidity control material (MOF-AHCM) was developed. Physicochemical and hygrothermal properties of the synthesized MOF-ACHM were characterized by experimental measurements. Full-scale chamber tests were conducted to analyze the moisture control capacity of the new material. Furthermore, numerical simulation was performed to investigate the energy-saving potential of MOF-AHCM on latent cooling load in different moisture climates worldwide. The main results are summarized as follows:

(1) MOF-AHCM exhibits an S-shaped water vapor isotherm characterized by steep adsorption and desorption occurring between 40 % and 60 % RH. In comparison to conventional hygroscopic materials, MOF-AHCM demonstrates excellent adsorption capacity (max. water uptake >0.56 g g^{-1}) and fast kinetics, while requiring a lower temperature for regeneration (50–60 °C).
(2) The full-scale chamber tests demonstrate that MOF-AHCM has exceptional moisture buffering ability (MBV >12 g m^{-2}·RH^{-1}) and can autonomously regulate indoor humidity within the optimal thermal comfort range (i.e., between 40 % and 60 % RH) without requiring additional energy input.
(3) Numerical simulations reveal that MOF-AHCM exhibits remarkable humidity control capabilities, thereby effectively diminishing the latent cooling loads in most climates worldwide. In arid, semiarid, and dry climates, the potential energy-saving rate for latent cooling loads can reach as high as 100 %. Moreover, even in moist climates, MOF-AHCM can achieve a substantial passive reduction in latent load, with rates of up to 55 %.
(4) In wet climates, MOF-AHCM should be coupled with an appropriate regeneration system to achieve indoor moisture control. MOF-AHCM has mild regeneration requirements, which can be easily attained using low-grade energy sources like solar energy.
(5) The MOF-AHCM synthesized in this paper is stable, safe, and has the potential for eco-friendly large-scale production.

In summary, MOF-based autonomous humidity control material is a promising candidate for energy-efficient humidity control in the built environment. By broadening our understanding of water adsorption in emerging porous materials and proposing innovative applications of these materials in buildings, this study opens new pathways for developing more sustainable and carbon-neutral technologies for built environment control.

CRediT authorship contribution statement

Menghao Qin: Writing – review & editing, Supervision, Methodology, Conceptualization. **Oliver S. Rasmussen:** Software, Investigation, Data curation. **Jun Chen:** Methodology, Formal analysis, Data curation. **Lars Wadsö:** Formal analysis, Data curation.

Declaration of competing interest

The authors declare that they have no known competing financial interests or personal relationships that could have appeared to influence the work reported in this paper.

Data availability

No data was used for the research described in the article.

Acknowledgments

The authors acknowledge the support from the Ingeniør, kaptajn Aage Nielsens fund. The authors thank D. Ding, K. Hansen, and E. Schnell for all the help in the experiments and Prof. Christian Serre from ENS Paris, France, for the helpful discussion.

Appendix A. Supplementary data

Supplementary data to this article can be found online at https://doi.org/10.1016/j.buildenv.2024.111757.

References

[1] H. Tabari, Climate change impact on flood and extreme precipitation increases with water availability, Sci. Rep. 10 (2020) 13768.
[2] IEA, The Future of Cooling, International Energy Agency Technical Report, Paris, 2018.
[3] G. Guarnieri, B. Olivieri, G. Senna, A. Vianello, Relative humidity and its impact on the immune system and infections, Int. J. Mol. Sci. 24 (11) (2023) 9456.
[4] S. Cui, M. Qin, A. Marandi, V. Steggles, S. Wang, et al., Metal-Organic Frameworks as advanced moisture sorbents for energy-efficient high temperature cooling, Sci. Rep. 8 (2018) 15284.
[5] X. Zheng, T. Ge, R. Wang, Recent progress on desiccant materials for solid desiccant cooling systems, Energy 74 (2014) 280–294.
[6] X. Liu, Y. Jiang, Temperature and Humidity Independent Control (THIC) of Air-Conditioning System, Springer, 2013.
[7] P.K. Tsobnang, E. Hastürk, D. Fröhlich, et al., Water vapor single-gas selectivity via flexibility of three potential materials for autonomous indoor humidity control, Cryst. Growth Des. 19 (5) (2019) 2869–2880.
[8] M. Zhang, M. Qin, C. Rode, Z. Chen, Moisture buffering phenomenon and its impact on building energy consumption, Appl. Therm. Eng. 124 (2017) 337–345.
[9] X. He, H. Zhang, L. Qiu, Z. Mao, C. Shi, Hygrothermal performance of temperature-humidity controlling materials with different compositions, Energy Build. 236 (2021) 110792.
[10] X. He, C. Feng, H. Zhang, Coupled heat and moisture transfer in walls featuring moisture-buffering materials and ventilating layers: an Experimental study, Energy Built Envir. 5 (1) (2024) 97–109.
[11] A. Lowenstein, Review of liquid desiccant technology for HVAC applications, HVAC R Res. 14 (2008) 819–839.
[12] J. Canivet, A. Fateeva, Y. Guo, B. Coasnecd, D. Farrusseng, Water adsorption in MOFs: fundamentals and applications, Chem. Soc. Rev. 43 (2014) 5594.
[13] K. Zu, M. Qin, S. Cui, Experimental and modeling investigation of water adsorption of hydrophilic carboxylate-based MOF for indoor moisture control, Energy 228 (2021) 120654.

[14] X. Jin, M.A. Medina, X. Zhang, Numerical analysis for the optimal location of a thin PCM layer in frame walls, Appl. Therm. Eng. 103 (2016) 1057–1063.
[15] M. Thommes, K. Kaneko, A.V. Neimark, et al., Physisorption of gases, with special reference to the evaluation of surface area and pore size distribution (IUPAC Technical Report), Pure Appl. Chem. 87 (2015) 1051–1069.
[16] ASHRAE, Ventilation for Acceptable Indoor Air Quality (ANSI/ASHRAE Standard 62.1-2010); American Society of Heating, Refrigerating, and Air Conditioning Engineers: Atlanta, GA, 2010.
[17] G. Férey, Hybrid porous solids: past, present, future, Chem. Soc. Rev. 37 (2008) 191–214.
[18] H. Furukawa, K. Cordova, M. O'Keeffe, O. Yaghi, The chemistry and applications of metal-organic frameworks, Science 341 (2013) 1230444.
[19] H. Kim, S. Yang, S. Rao, S. Narayanan, A. Umans, O. Yaghi, E. Wang, et al., Water harvesting from air with metal-organic frameworks powered by natural sunlight, Science (Apr) (2017).
[20] X. Feng, M. Qin, S. Cui, et al., Metal-organic framework MIL-100 (Fe) as a novel moisture buffer material for energy-efficient indoor humidity control, Build. Environ. 145 (2018) 234–242.
[21] K. Zu, M. Qin, S. Cui, Progress and potential of metal-organic frameworks (MOFs) as novel desiccants for built environment control: a review, Renew. Sustain. Energy Rev. 133 (2020) 110246.
[22] P. Hou, K. Zu, M. Qin, S. Cui, A novel metal-organic frameworks based humidity pump for indoor moisture control, Build. Environ. 187 (2021) 107396.
[23] M. Qin, O. Feaugas, K. Zu, Novel metal-organic framework (MOF) based phase change material composite and its impact on building energy consumption, Energy Build. 273 (2022) 112382.
[24] X. Zhang, C. Li, A. Chinnappan, S. Zheng, Z. Sun, C. Baskar, S. Ramakrishna, MOFs for handling latent load in air cooling: from moisture adsorption and optimization to application as heat exchanger coatings in air conditioners, Coord. Chem. Rev. 495 (2023) 215384.
[25] D. Ding, M. Qin, Metal–organic frameworks (MOFs) based electrospun nanofiber membrane for passive indoor moisture control, Buildings 13 (2023) 1192.
[26] R.G. AbdulHalim, P.M. Bhatt, Y. Belmabkhout, A. Shkurenko, et al., A fine-tuned metalorganic framework for autonomous indoor moisture control, J. Am. Chem. Soc. 139 (2017) 10715–10722.
[27] S.M.T. Abtab, D. Alezi, P.M. Bhatt, A. Shkurenko, , et al.Nejib Hedhili Mohamed, Eddaoudi Mohamed, Reticular chemistry in action: a hydrolytically stable MOF capturing twice its weight in adsorbed water, Chem 4 (1) (2018) 94–105.
[28] M. Qin, P. Hou, Z. Wu, J. Wang, Precise humidity control materials for autonomous regulation of indoor moisture, Build. Environ. 169 (2020) 106581.
[29] D. Ma, P. Li, X. Duan, J. Li, P. Shao, Z. Lang, L. Bao, et al., A hydrolytically stable vanadium(IV) metalorganic framework with photocatalytic bacteriostatic activity for autonomous indoor humidity control, Angew. Chem., Int. Ed. Engl. 59 (2020) 3905–3909.
[30] J. Zhang, P. Li, X. Zhang, X. Ma, B. Wang, Aluminum metal-organic frameworks with photocatalytic antibacterial activity for autonomous indoor humidity control, ACS Appl. Mater. Interfaces 12 (2020) 46057–46064.
[31] C. Ho, M.L. Valentine, Z. Chen, et al., Structure and thermodynamics of water adsorption in NU-1500-Cr, Commun. Chem. 6 (2023) 70.
[32] N. Zhu, Z. Wei, C. Chen, X. Xiong, Y. Xiong, Z. Zeng, et al., High water adsorption MOFs with optimized pore-nanospaces for autonomous indoor humidity control and pollutants removal, Angew. Chem., Int. Ed. Engl. 61 (2022) e202112097.
[33] T.J. Matemb Ma Ntep, M. Wahiduzzaman, E. Laurenz, I. Cornu, G. Maurin, C. Janiak, C. Serre, et al., When polymorphism in metal–organic frameworks enables water sorption profile tunability for enhancing heat allocation and water harvesting performance, Adv. Mater. (2023) 2211302.
[34] R. Cimino, K.A. Cychosz, M. Thommes, A. Neimark, Experimental and theoretical studies of scanning adsorption-desorption isotherms, Colloids Surf. A Physicochem. Eng. Asp. 437 (2013).
[35] Z. Chen, M. Qin, J. Yang, Synthesis and characteristics of hygroscopic phase change material: composite microencapsulated phase change material (MPCM) and diatomite, Energy Build. 106 (2015) 175–182.
[36] C. Rode, Moisture Buffering of Building Materials, Department of Civil Engineering, Technical University of Denmark, 2005.
[37] K. Zu, M. Qin, C. Rode, M. Libralato, Development of a moisture buffer value model (MBM) for indoor moisture prediction, Appl. Therm. Eng. 171 (2020) 115096.
[38] D. Ding, O.S. Rasmussen, M. Qin, Moisture buffer value for hygroscopic materials with different thicknesses, Build. Environ. 258 (2024) 111581.
[39] K. Zu, Metal-organic Frameworks (MOFs) for Energy-Efficient Indoor Moisture Control: Synthesis, Characterization and Applications, PhD Thesis, The Technical University of Denmark, Denmark, 2021.
[40] Z. Chen, M. Qin, Preparation and hygrothermal properties of composite phase change humidity control materials, Appl. Therm. Eng. 98 (2016) 1150–1157.
[41] M.I. Severino, E. Gkaniatsou, F. Nouar, M.L. Pinto, C. Serre, MOFs industrialization: a complete assessment of production costs, Faraday Discuss 231 (2021) 326–341.
[42] T. Padfield, The Role of Absorbent Building Materials in Moderating Changes of Relative Humidity, PhD Thesis, The Technical University of Denmark, Denmark, 1999.
[43] V. Cascione, D. Maskell, A. Shea, P. Walker, The moisture buffering performance of plasters when exposed to simultaneous sinusoidal temperature and RH variations, J. Build. Eng. 34 (2021) 101890.
[44] K. Wittchen, K. Johnsen, K. Grau, BSIM User's Guide, Danish Building Research Institute, Hørsholm, Denmark, 2005.
[45] C. Pedersen, Prediction of moisture transfer in building constructions, Build. Environ. 27 (1992) 387–397.
[46] C.P. Rode, Combined Heat and Moisture Transfer in Building Constructions, PhD Thesis, Technical University of Denmark, 1990.
[47] M. Libralato, A. De Angelis, O. Saro, M. Qin, C. Rode, Effects of considering moisture hysteresis on wood decay risk simulations of building envelopes, J. Build. Eng. 42 (2021) 102444.
[48] J.J. Feddema, A revised thornthwaite-type global climate classification, Phys. Geogr. 26 (6) (2005) 442–466.
[49] Tao Zhang, Xiaohua Liu, Yi Jiang, Development of temperature and humidity independent control (THIC) air-conditioning systems in China—a review, Renew. Sustain. Energy Rev. 29 (2014) 793–803.
[50] ANSI/ASHRAE Addendum P to ANSI/ASHRAE Standard 62.1-2013, Ventilation for Acceptable Indoor Air Quality, ASHRAE Standards Committee, 2015.
[51] H. Kunzel, Simultaneous Heat and Moisture Transport in Building Components, Ph. D. Thesis, Fraunhofer Institute of Building Physics, German, 1995.
[52] D. Ding, O.S. Rasmussen, M. Qin, Sustainable metal-organic framework based paper sheet as wallpaper for passive indoor moisture control, Energy Build. 313 (2024) 114262.
[53] J. Jacobs, C.E. Deering, R. Sui, K.L. Lesage, Degradation of desiccants in temperature swing adsorption processes: the temperature dependent degradation of zeolites 4A, 13X and silica gels, Chem. Eng. J. 451 (2023) 139049.
[54] Ş. Sayılgan, M. Mobedi, S. Ülkü, Effect of regeneration temperature on adsorption equilibria and mass diffusivity of zeolite 13x-water pair, Microporous Mesoporous Mater. 224 (2016) 9–16.
[55] K. Zu, S. Cui, M. Qin, Performance comparison between metal-organic framework (MOFs) and conventional desiccants (silica gel, zeolite) for a novel high temperature cooling system, IOP Conf. Ser. Mater. Sci. Eng. 609 (2019) 052013.
[56] C. Sun, Y. Zhu, P. Shao, L. Chen, X. Huang, S. Zhao, et al., 2D covalent organic framework for water harvesting with fast kinetics and low regeneration temperature, Angew. Chem. Int. Ed. 135 (2023) e202217103.